Available online at www.sciencedirect.com
ScienceDirect
Journal of the European Ceramic Society 27 (2007) 2223–2228
www.elsevier.com/locate/jeurceramsoc

Preparation of ordered porous SnO_2 films by dip-drawing method with PS colloid crystal templates

Yanan Fu, Zhengguo Jin *, Zhifeng Liu, Wei Li

Key Laboratory for Advanced Ceramics and Machining Technology of Ministry of Education, School of Materials, Tianjin University, 300072 Tianjin, PR China

Received 11 January 2006; received in revised form 8 July 2006; accepted 15 July 2006
Available online 8 September 2006

Abstract

Ordered macroporous SnO_2 thin films were fabricated by using colloid crystal template of polystyrene (PS) spheres. Efficient dip-drawing method was used in both PS template assembly and the fabrication of porous structure. The PS templates were orderly assembled on clean glass substrates through colloid crystallization of monodisperse PS latex spheres, which were synthesized by an emulsion polymerization technique. The porous SnO_2 thin films were prepared through filling SnO_2 precursor sol into the spaces among the close-packed PS templates, and then annealing at 500 °C to remove the PS spheres and form SnO_2 crystal wall. The forming mechanism of PS templates through dip-drawing method was explained based on three driving forces existing in the assembly processes. The SnO_2 sol concentration and PS sphere size had important effects on formation of ordered porous structure The X-ray diffraction (XRD) spectra indicated the thin film was rutile structure and consisted of nanometer grains. The transmittance spectrum showed that optical transmittance kept above 80% beyond the wavelength of 440 nm. Optical band-gap of the porous SnO_2 film was 3.68 eV.

Keywords: Dip-drawing method; Porosity

1. Introduction

Ordered macroporous (>50 nm) materials have recently received much attention due to their potential application in various areas of separation processes, catalysis, photonic band-gap (PBG) materials, and other emerging nanotechnologies.[1] Various methods are available for producing this kind of materials, for example, electrochemical and chemical etching,[2] methods based on foaming of emulsion solutions,[3] sintering of ceramic particles,[4] and methods based on assembly of block copolymers.[5] Considerable advantages are being made in the template-assisted assembly of macroporous materials. Colloidal crystalline arrays based on ordered aggregation of spherical-silica or latex-polymer nanoparticles (polystyrene (PS) or poly (methyl methacrylate) (PMMA)) have been used as templates for synthesizing new macroporous materials, including inorganic materials,[6] metals,[7] polymers,[8] and carbons.[9] With this method, a colloid crystal array is first assembled from a solution containing template material by gravity sedimentation method,[10] vertical deposition[11] or evaporation of the emulsion with a tilted system,[12] and then impregnated with the desired solid material. Finally, the template is removed, resulting in an array of macropores that reflects the structure of the template. However, these template assembly methods generally need long operating period and strict surrounding conditions, such as, temperature, humidity and resistance to vibration.

In new type photovoltaic solar cells such as dye-sensitized solar cells (DSSCs) and extremely thin absorber solar cells (ETAs), the photoanode films require high specific surface area so as to deposit more absorber in order to obtain high photon-to-current conversion efficiency. Ordered macroporous films have been considered as a sort of promising photoanodes because of their uniform microstructure and convenient control of both pore size and nanograin size.[13] Stannic oxide, with a wide band-gap of 3.62 eV and higher transparence than TiO_2 over shorter wavelength range, could be used as a substitute of TiO_2 anode in solar cells. Moreover, SnO_2 holds high electrical conductivity (8×10^{-4} Ωcm) and chemical stability. Stannic oxide

* Corresponding author. Tel.: +86 22 27890266; fax: +86 22 27404724.
E-mail address: zhgjin@tju.edu.cn (Z. Jin).

0955-2219/$ – see front matter © 2006 Elsevier Ltd. All rights reserved.
doi:10.1016/j.jeurceramsoc.2006.07.006

films have been fabricated by a number of techniques, mainly including spray pyrolysis,[14] sputtering,[15] chemical vapour deposition (CVD),[16] evaporation[17] and sol–gel technique,[18] in which sol–gel technique presents several advantages[19]: excellent homogeneity, easy control of film thickness, ability to coat large and complex shapes, and low-temperature and low-cost processing. As the photoanode of the new type solar cells, SnO_2 nanocrystal film should have ordered macroporous structure and high optical transmittance in the range of visible light with a wide band-gap.

In this paper, we have chosen a dip-drawing method to assemble monolayer PS array templates, which only needs very short period of operating process. Meanwhile, we prepared SnO_2 precursor sol and pour it in the spaces between PS sphere array templates also by the dip-drawing method. The mechanism of template assembly was discussed. Phase composition, optical properties and the influences of SnO_2 precursor concentration together with PS sphere size on structural characteristics of the porous films were investigated.

2. Experimental procedure

2.1. Chemicals

In the preparation of PS spheres emulsion and SnO_2 sol, the following materials were used: styrene (C_8H_8, AR), potassium persulfate ($K_2S_2O_8$, AR), sodium dodecyl sulfate (SDS, AR), Sodium bicarbonate ($NaHCO_3$, AR), 0.1 mol/L sodium hydroxide (NaOH, AR), stannous chloride dihydrate ($SnCl_2{\cdot}2H_2O$, AR), ethanol (CH_3CH_2OH, AR) and deionized water.

2.2. Synthesis

2.2.1. Synthesis of monodisperse PS spheres

Non-crosslinked, monodisperse PS spheres were synthesized by emulsion polymerization technique. A five-necked, 1000 mL round-bottomed flask was filled with 250 mL deionized water and 0.01 g SDS. The system was heated to 70 °C, stirred at about 300 rpm and purged with argon in order to eliminate the inhibition effect of oxygen. Styrene (40 mL) was washed with 0.1 M NaOH solution and deionized water in turn for four times in order to remove polymerization inhibitor. $NaHCO_3$ (0.2 g) was used as buffer. Then styrene monomer was introduced. In a separate beaker, $K_2S_2O_8$ initiator with 50 mL water was heated to 70 °C, then added into the flask. Two quantities of initiators were employed to fabricate PS spheres with different sizes. The polymerization was continued for 13 h and the resulting latex spheres were remained suspended in their mother liquor until used.

2.2.2. Assembly of the PS array templates

The PS array templates were firstly assembled by dip-drawing method. The microslides as substrates were cleaned ultrasonically in acetone, hydrochloric acid (pH 2), ethanol and deionized water in turn, soaked in sodium hydroxide solution for 30 min and then preserved in ethanol. The clean glass substrate was settled vertically into the emulsion of PS spheres for several minutes, and then slowly drawn out from the emulsion with a drawing rate of 0.2 cm/min and dried in oven at 30 °C for 20 min. The PS templates appeared opalescent, as expected, prismatic colours like rainbow, depending on the angle of observation, and clearly visible when the samples were illuminated from above with white light.

2.2.3. Synthesis of SnO_2 sol

SnO_2 precursor sol was prepared in the following way: $SnCl_2{\cdot}2H_2O$ was dissolved in absolute ethanol. The solution was stirred magnetically and simultaneously with reflux at 80 °C for 2 h. After cooling, the solution was aged at room temperature for 24 h. Then a uniform and transparent $Sn(OC_2H_5)_n$ sol was obtained for film fabrication.

2.2.4. Preparation of ordered porous SnO_2 films

The dip-drawing method was also used to fill the SnO_2 sol on the PS sphere templates; the template was kept in the sol for 3 min and the drawing rate was 3 cm/min. When the templates entered the sol, the precursor sol could permeate the spaces of close-packed PS array templates by capillary force and form a gel skeleton around the spheres when drawing out from the sol. The templates were placed into four different concentrations of the SnO_2 sols (0.1∼0.8 mol/L). The templates poured were dried in oven at 30 °C for 1 h, and then electrically heated in air up to 500 °C for 1 h at a heating rate of 2 °C/min to remove the PS templates and obtain porous structure of SnO_2 thin films.

2.3. Characterization

The diameters of PS spheres were estimated by using transmission electron microscopy (TEM). The morphology of porous films was observed by using a PHILIPS XL-30 environment scanning electron microscopy (ESEM). X-ray diffraction (XRD) patterns of SnO_2 thin films were recorded with Rigaku D/max-2500 using Cu Kα radiation ($\lambda = 0.154059$ nm). The optical transmittance was detected by DU-8B UV–vis double-beam spectrophotometer.

3. Results and discussion

3.1. PS colloidal crystal templates

Fig. 1 shows the TEM images of PS spheres, which were synthesized by the emulsion polymerization technique mentioned above. Their average diameters are 330 and 400 nm with dispersion smaller than 2%.

Fig. 2 shows the schematic outline of the dip-drawing method, which was used to assemble PS colloidal crystal templates. In the process of array template formation, when the wettable substrate was dipped into the emulsion, a meniscus water–substrate–air interface system formed, which was caused by wetting effect. So it could be expected that there were three driving forces which attributed to the assembly of the array template. The first one was adsorption force of substrate surface to PS spheres dispersed in the emulsion. The second was floatation force of solvent near the meniscus region which applied to the PS spheres under the liquid surface of emulsion. It combined with the adsorption

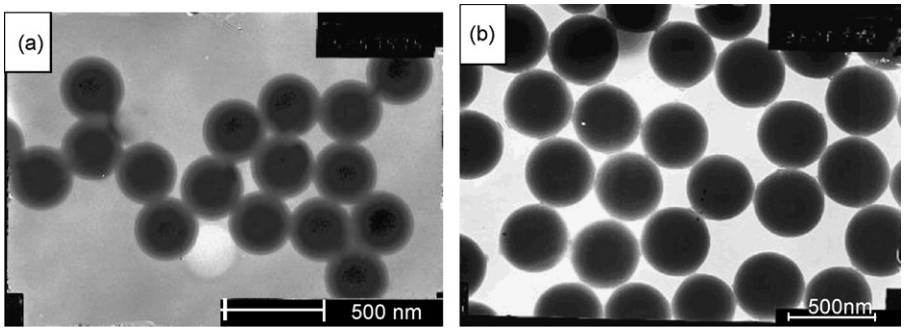

Fig. 1. TEM images of polystyrene spheres.

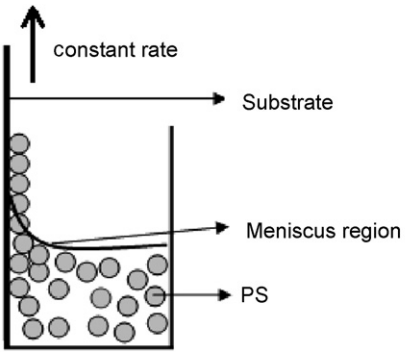

Fig. 2. Schematic outline of template assembly by dip-drawing method.

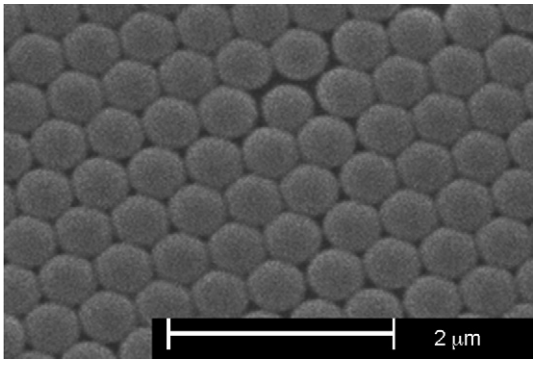

Fig. 3. SEM image of PS array template with diameter of 330 nm in monolayer.

force to make the spheres stick to the substrate surface even at liquid height of the meniscus region. The third was capillary force between the spheres as well as sphere and substrate while the spheres were drawn up from the emulsion. This force made the formation of colloid crystal nucleus, close package of array and adherence of PS spheres to the substrate. The formation of ordered array template mainly depends on drawing rate, solvent evaporation, and thermal diffusion of spheres in the emulsion, in which the drawing rate stands as a parameter to be controlled easily. Over-high drawing rate will lead to faster PS sphere crystallization and shorter action time of capillary forces, resulting in the decrease of ordered structure perfection.

Fig. 3 shows the surface image of PS colloid crystal template prepared by the dip-drawing method, exhibiting a close-packed, ordered and hexagonal arrangement of polystyrene spheres with each sphere touching six others in one layer, but there are still some defects at small local parts.

3.2. Formation of porous SnO_2 films

Fig. 4 shows the preparation process of SnO_2 thin films by the dip-drawing method. The substrate with colloid crystal template was settled vertically into the sol. The precursor sol permeated the spaces of close-packed PS array template by capillary force. Then, the PS template imbued with SnO_2 sol was drawn out and the porous SnO_2 thin film was obtained after removing the PS by heat treatment.

The dip-drawing method has some advantages than the vertical pouring method employed by others.[20,21] Both methods

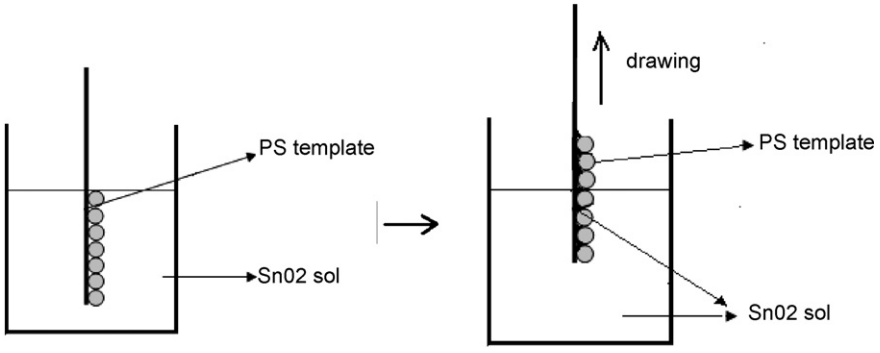

Fig. 4. Schematic chart of dip-drawing method.

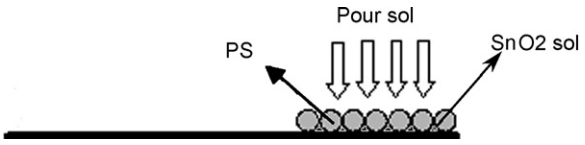

Fig. 5. Schematic chart of vertical pouring way.

are showed in Figs. 4 and 5, respectively. It is easy to see that the vertical pouring method is difficult to control the required content of precursor when the template is horizontally placed. More precursor sol will submerge the PS spheres template. On the contrary, deficient precursors will not fully pour the spaces of template. In the dip-drawing method, filling content of SnO_2 sol can be balanced by capillary force and gravity, leading to a stable filling content.

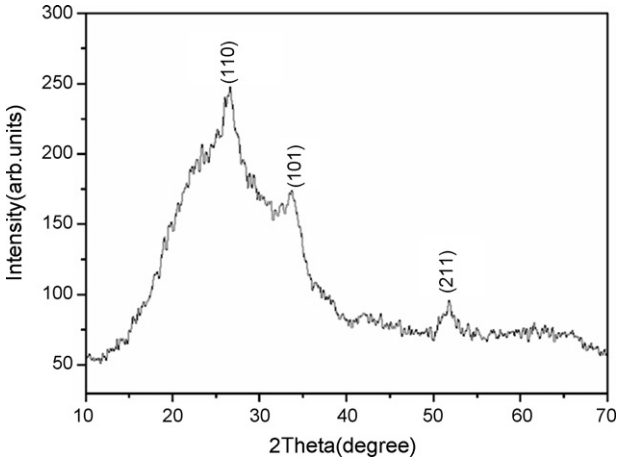

Fig. 6. XRD pattern of SnO_2 film fired at 500 °C for 1 h.

3.3. Structure characteristics of porous SnO_2 films

Fig. 6 shows X-ray diffraction spectra of the porous SnO_2 thin films fired at temperature 500 °C for 1 h. Obvious peaks can be observed at $2\theta = 26.6°$, 33.5° and 51.7°, corresponding to (1 1 0), (1 0 1), (2 1 1) reflections of the rutile structure, respectively. Furthermore, the average grain size D of SnO_2 was estimated according to XRD HFMW (half full maximum width) method, based on Scherrer formula:

$$D = \frac{K\lambda}{(\beta \cos\theta)}$$

where K is the shape factor of the average crystallite (expected shape factor is 0.9), λ the wavelength (usually 1.54056 Å for Cu Kα1), β the full width at half maximum (FWHM) and θ is the peak position, giving about 10 nm average grain size for (1 1 0).

3.4. Morphology of porous SnO_2 films

Fig. 7 shows the influence of sol concentration on the morphology of porous SnO_2 thin films. As showed in Fig. 7(a), lower concentration of SnO_2 sol (0.1 mol/L) induces the following result: the inorganic wall can be formed but relatively thin and the array template is partly destroyed. It indicates that lower concentration has better permeation but a tendency to destroy the order level of the template due to the action of lower viscosity combined with higher specific gravity of sol than the PS emulsion when the substrate is drawn up. Fig. 7(d) shows the morphology of thin films with sol concentration of 0.8 mol/L. It can be seen that sphere shell array of SnO_2 solid appears after the removing of PS spheres. The reason may be that SnO_2 sol with higher concentration and viscosity fills the spaces among PS spheres, while covers the sphere surface with enough thickness

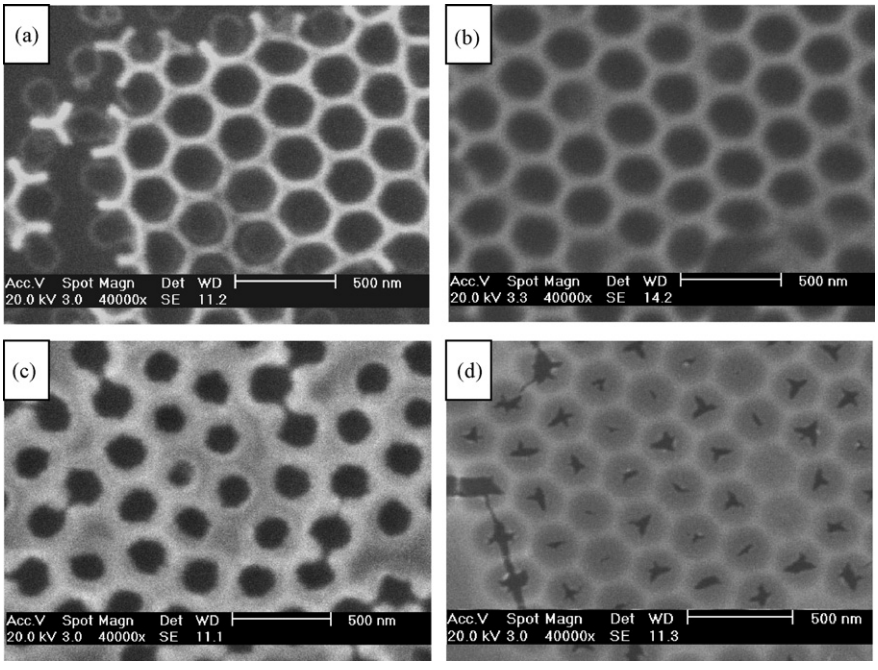

Fig. 7. SEM images of thin films with different sol concentrations.

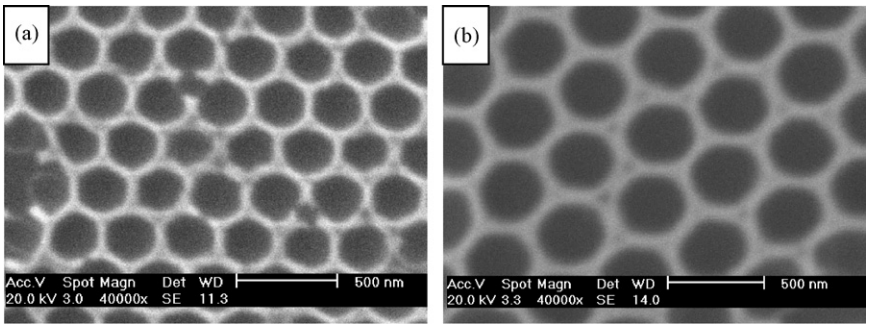

Fig. 8. SEM images of thin films with different template sphere sizes.

of layer so as to stand the shape after removing the spheres. In conclusion, sol concentration plays a key role in the formation of ordered porous SnO_2 films. In this experiment, the suitable sol concentrations, which have a satisfactory permeation and viscosity and can form 'honeycomb' structure, are over the range of 0.2–0.4 mol/L.

Fig. 8 shows the influence of sphere sizes of colloid crystal template on the morphology of SnO_2 porous thin films (SnO_2 sol concentration is 0.25 mol/L). It can be seen that structure defects of the inorganic wall from small sphere array are more remarkable. It implies that choice of the sol concentration used should match to the sphere size: bigger sphere template has better permeation and higher sol concentration can be employed; contrarily, lower concentration is suitable to the small sphere template in order to obtain a good pouring structure.

It should be noted that the pore diameter depends on the size of PS spheres used and the sol concentration. Typically, for the 0.25 mol/L sol, the average pore diameters of SnO_2 thin films are about 232 nm for sphere diameter 330 nm (Fig. 8(a)) and around 320 nm for sphere diameter 400 nm (Fig. 8(b)), corresponding to the shrinkage ratio is 29.7 and 21.0%, respectively. The bigger sphere size corresponds to less shrinkage, showing better filling quality among the spaces of spheres.

For the hexagonal single-layer porous structure model, showed in Fig. 9, the area of formed porous surface is $3\pi r^2 + 6\sqrt{3}r^2$ corresponding to the area of plane surface $6\sqrt{3}r^2$(where r is the radius of spheres), so the ratio of both areas is a constant and equals to 1.924, no matter how much the sphere size is. It indicates that it is limited to increase the surface areas of porous structure by using smaller spheres.

3.5. Optical characteristics of porous SnO_2 films

Fig. 10 shows optical transmittance in the wavelength (λ) range 300–900 nm for the porous SnO_2 film prepared from 330 nm sphere template, and a dense one is also showed as a reference. From these, it can be seen that the optical transmittance could keep a high level (above 80%) beyond the wavelength of 440 nm for both porous film and dense one. Moreover, the transmission of porous sample is about 5% lower than the dense one over the range of 550–850 nm. This indicates that porous structure increases the interface scattering, which results in a little decrease of transmission over the visible wavelength range. The sharp absorption onset of the SnO_2 at wavelengths above 440 nm is nearly the same for both porous and dense films. Thus, porous structure has little effect on the optical transmittance of SnO_2 films.

The absorption coefficient α is given by the transmittance T and film thickness d using the formula $\alpha = -\ln(T)/d$. The dependence of the absorption coefficient α upon the photon energy $h\nu$ for near edge optical absorption in semiconductors takes the form $\alpha h\nu = k(h\nu - E_g)^m$, Where E_g is the optical band-gap, k is a constant and $m = 1/2$ for SnO_2 with an allowed direct energy gap. A typical $(\alpha h\nu)^2$ was plotted versus $h\nu$ using the data obtained from the optical absorption spectra (Fig. 11). The band-gaps

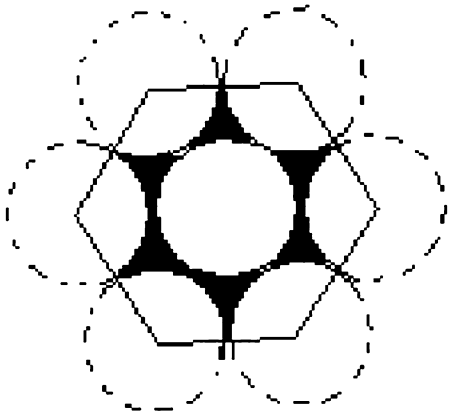

Fig. 9. Hexagonal single-layer porous structure model.

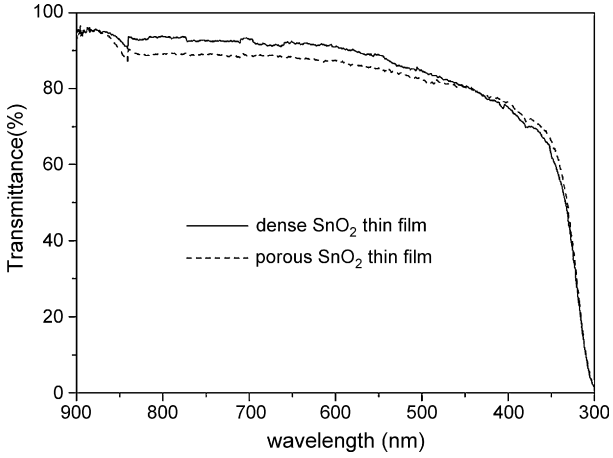

Fig. 10. Optical transmittance spectra of SnO_2 thin films.

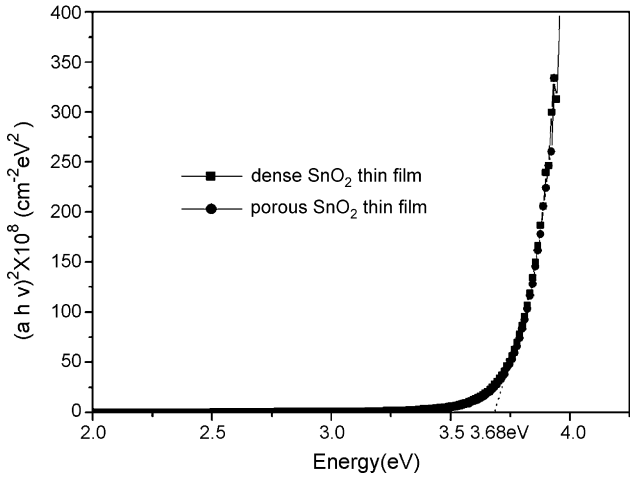

Fig. 11. Plot of $(\alpha h\nu)^2$ vs. $h\nu$ for the SnO_2 films.

of porous and dense samples are nearly the same, which is accordant with the same transmission near shorter wavelength (Fig. 10). So it is found that the dependence of the energy gap for stannic oxide on the porous or dense structure is not strong. The band-gap of as-prepared porous SnO_2 thin film is 3.68 eV, so the wide band-gap SnO_2 film could be used as the photoanode in solar cells.

4. Conclusion

The close-packed monolayer arrays of PS templates were successfully assembled on clean glass substrates by dip-drawing method from the emulsion of PS spheres. Porous SnO_2 thin films were prepared by filling the SnO_2 sol into the spaces of close-packed PS spheres templates with dip-drawing method and then annealing to remove the PS templates. The results showed that for 330 nm PS colloid crystal templates ordered 'honeycomb' SnO_2 structure could be obtained with sol concentration over the range of 0.2–0.4 mol/L. And SnO_2 sol with higher concentration could be applied to bigger PS sphere templates. The thin films were rutile structure observed by X-ray diffraction spectra. And the transmittance spectrum indicated that optical transmittance kept a high level (above 80%) beyond the wavelength of 440 nm. Optical band-gaps of SnO_2 film (fired at 500 °C) were 3.68 eV.

Acknowledgement

The authors (Z.G. Jin, Y.N. Fu) gratefully acknowledge financial support from Natural Science Foundation of Tianjin (No. 033802311).

References

1. Velev, O. D. and Lenhoff, A. M., Colloidal crystals as templates for porous materials. *Curr. Opin. Colloid Interface Sci.*, 2000, **5**, 56–63.
2. Searson, P. C., Porous silicon membranes. *Appl. Phys. Lett.*, 1991, **59**, 832–833.
3. Even Jr., W. R. and Gregory, D. P., Emulsion-derived foams: preparation, properties and application. *MRS Bull.*, 1994, **XIX**(4), 29–33.
4. Leenaars, A. F. M., Keizer, K. and Burggraaf, A. J., *CHEMTECH*, February 1986, 560–564.
5. Widawski, G., Rawiso, M. and Francüois, B., Self-organized honeycomb morphology of star-polymer polystyrene films. *Nature*, 1994, **369**, 387–389.
6. Sung, I. K., Yoon, S. B. and Yu, J. S., Fabrication of macroporous SiC from templated preceramic polymers. *Chem. Commun.*, 2002, 1480–1481.
7. Kulinowski, K. M., Jiang, P. and Vaswani, H., Porous metals from colloidal templates. *Adv. Mater.*, 2000, **12**, 833–838.
8. Miguez, H., Meseguer, F. and Lopez, C., Synthesis and photonic bandgap characterization of polymer inverse opals. *Adv. Mater.*, 2001, **13**, 393.
9. Kang, S., Yu, J.-S. and Kruk, M., Synthesis of an ordered macroporous carbon with 62 nm spherical pores that exhibit unique gas adsorption properties. *Chem. Commun.*, 2002, 1670–1671.
10. Bartlett, P. N., Baumberg, J. J. and Birkin, P. R., Highly ordered macroporous gold and platinum films formed by electrochemical deposition through templates assembled from submicron diameter monodisperse polystyrene spheres. *Chem. Mater.*, 2002, **14**, 2199–2208.
11. Ye, Yonghong, LeBlanc, F. and Hache, A., Self-assembling three-dimensional colloidal photonic crystal structure with high crystalline quality. *Appl. Phys. Lett.*, 2001, **78**, 52–54.
12. Micheletto, R., Fukuda, H. and Ohtsu, M., A simple method for the production of a two-dimensional, ordered array of small latex particles. *Langmuir*, 1995, **11**, 3333–3336.
13. Zukalova, M., Zukal, A. and Kavan, L., Organized mesoporous TiO_2 films exhibiting greatly enhanced performance in dye-sensitized solar cells. *Nano Lett.*, 2005, **5**(9), 1789–1792.
14. Shanti, E., Duttta, V. and Chopra, K. L., Electrical and optical properties of undoped and antimony-doped tin oxide films. *J. Appl. Phys.*, 1980, **51**, 6243–6251.
15. Karasawa, T. and Miyata, Y., Electrical and optical properties of indium tin oxide thin films deposited on unheated substrates by dc reactive sputtering. *Thin Solid Films*, 1993, **223**, 135–139.
16. Tarey, R. D. and Raju, T. A., A method for the deposition of transparent conducting thin films of tin oxide. *Thin Solid Films*, 1985, **128**, 181–189.
17. Lane, D. W., Coath, J. A. and Beldon, H. S., Optical properties and structure of thermally evaporated tin oxide films. *Thin Solid Films*, 1992, **221**, 262–266.
18. Park, S. S. and Mackenzie, J. D., Sol–gel-derived tin oxide thin films. *Thin Solid Films*, 1995, **258**, 268–273.
19. Klein, L. C., *Sol-Gel technology for thin films, fibers, preforms, electronics and specialty shapes*. Noyes Publications, Park Ridge, New Jersey, 1988.
20. Shen, Y., Wu, Q. Z. and Liao, J. F., *J. Inorg. Mater.*, 2003, **18**, 401.
21. Wu, Q. Z., Shen, Y., Sun, Z. F. and Li, Y. G., *J. Inorg. Mater.*, 2004, **19**, 39.